# Response of North American Great Basin Lakes to Dansgaard–Oeschger oscillations

Larry Benson
*University of Colorado at Boulder*, great.basin666@gmail.com

Steve Lund
*University of Southern California*, slund@usc.edu

Robert M. Negrini
*California State University - Bakersfield*, rnegrini@csub.edu

Braddock Linsley
*State University of New York*

Mladen Zic
*California State University - Bakersfield*

PERGAMON

Quaternary Science Reviews 22 (2003) 2239–2251

QSR

# Response of North American Great Basin Lakes to Dansgaard–Oeschger oscillations

Larry Benson[a,*], Steve Lund[b], Rob Negrini[c], Braddock Linsley[d], Mladen Zic[c]

[a] US Geological Survey, 3215 Marine Street, Boulder, CO 80303-1066, USA
[b] Department of Earth Sciences, University of Southern California, Los Angeles, CA 90089, USA
[c] Department of Physics and Geology, California State University, Bakersfield, CA 93311, USA
[d] Earth and Atmospheric Sciences, State University of New York, 1400 Washington Avenue, Albany, NY 12222, USA

Received 15 January 2003; accepted 10 June 2003

**Abstract**

We correlate oscillations in the hydrologic and/or cryologic balances of four Great Basin surface-water systems with Dansgaard–Oeschger (*D–O*) events 2–12. This correlation is relatively strong at the location of the magnetic signature used to link the lake records, but becomes less well constrained with distance/time from the signature. Comparison of proxy glacial and hydrologic records from Owens and Pyramid lakes indicates that Sierran glacial advances occurred during times of relative dryness. If our hypothesized correlation between the lake-based records and the GISP2 $\delta^{18}O$ record is correct, it suggests that North Atlantic D–O stades were associated with relatively cold and dry conditions and that interstades were associated with relatively warm and wet conditions throughout the Great Basin between 50,500 and 27,000 GISP2 yr B.P. The Great Basin lacustrine climate records reinforce the hypothesis that D–O events affected the climate throughout much of the Northern Hemisphere during marine isotope stages 2 and 3. However, the absolute phasing between lake-size and ice-core $\delta^{18}O$ records remains difficult to determine.
Published by Elsevier Ltd.

## 1. Introduction

During the past decade, high-resolution $\delta^{18}O$ data sets from the Greenland ice sheet (Johnsen et al., 1992, 1997; Grootes and Stuiver, 1997; Stuiver and Grootes, 2000) have permitted recognition of 24 interstades within the last glacial cycle (Dansgaard et al., 1993). Each interstade begins with a large and abrupt increase in $\delta^{18}O$ (warming), usually followed by a much slower transition (cooling) to a $\delta^{18}O$ minima. These stadial–interstadial oscillations have become known as Dansgaard–Oeschger (*D–O*) cycles.

Bond et al. (1993) were the first to link ice and marine records, showing that proxy sea-surface temperature (SST) records from two North Atlantic sediment cores could be correlated to match the Greenland $\delta^{18}O$ record. They noted that millennial-scale D–O cycles were bundled into longer-duration cooling cycles, each terminated by an abrupt shift from cold to warm temperatures. Exceptionally large discharges of icebergs known as Heinrich events (Heinrich, 1988; Broecker et al., 1992) occurred near some of the terminations.

Since 1993, a variety of other proxy-climate records from both marine and continental sites have been linked to the GISP2 $\delta^{18}O$ record. Rasmussen et al. (1996) showed that magnetic susceptibility and foraminiferal assemblage variations in a sediment core taken from the coastal margin north of the Faroe Islands could be matched to D–O events 3–15. Gentry et al. (2003) found rapid climate oscillations coincident with D–O events between 83,000 and 32,000 yr ago, using the $\delta^{18}O$ and $\delta^{13}C$ records of a stalagmite collected in southwest France. Farther south in the subtropical North Atlantic, Sachs and Lehman (1999) matched oscillations in alkenone-derived SST records to D–O events 5–17, using changes in sediment lightness, a proxy for $CaCO_3$ content that had been previously linked to the GISP2 $\delta^{18}O$ record (Boyle, 1997). In the tropical Atlantic Cariaco Basin, Hughen and colleagues (Hughen et al., 1996; Peterson et al., 2000) linked records of marine productivity, precipitation, and South American river discharge to D–O events 1–21. Altabet et al. (2002) showed that oscillations in $\delta^{15}N$, %N, and total chlorines in sediment cores taken from the Arabian

*Corresponding author. Tel.: +1-303-541-3005; fax: +1-303-447-2505.
*E-mail address:* lbenson@usgs.gov (L. Benson).

0277-3791/$ - see front matter Published by Elsevier Ltd.
doi:10.1016/S0277-3791(03)00210-5

Sea corresponded to D–O events 1–17, suggesting that atmospheric forcing of Northern Hemisphere climate altered the intensity of upwelling associated with the summer monsoon. And in eastern China, stalagmites from the Nanjing area indicate $\delta^{18}O$ oscillations that appear to correspond to D–O events 1–21, suggesting a strong correspondence of East Asian Monsoon intensity with Greenland air temperature (Wang et al., 2001). In the western tropical Pacific, Stott et al. (2002) have argued, using $\delta^{18}O$ and the Mg/Ca compositions of planktonic foraminifera, that the salinity of the Pacific warm pool has varied in accordance with D–O events 1–19. Salinities were higher at times of high-latitude cooling (D–O stades) and lower during interstades. On the California margin, Behl and Kennett (1996), Hendy and Kennett (1999) and Hendy et al. (2002) have correlated changes in lamination style, planktonic $\delta^{18}O$, and foraminiferal assemblages in core ODP 893A with the GISP2 $\delta^{18}O$ record. Heusser (1998) analyzed pollen from the same core and showed that several sea-surface warming events were accompanied by increases in plants such as oak that prefer a warm climate. In addition, Seki et al. (2002) have determined that alkenone-based SSTs record D–O and Heinrich events in a marine core taken offshore of Point Conception, California.

Thus, several Northern Hemisphere records indicate the presence of D–O cycles, although in most cases, neither the synchroneity of such events nor their point of origin have yet been unequivocally demonstrated. Recently, Hinnov et al. (2002) have shown that D–O cycles also occur in southern ice-core records. This study appears to demonstrate that the temperature perturbation accompanying D–O events is global in scale, although the perturbation in the Southern Hemisphere has only ~1/10th the power of the perturbation in the Northern Hemisphere.

In this paper, we attempt to add an additional link to the chain of studies that demonstrate that D–O cycles affected the climate of much and perhaps all of the Northern Hemisphere. Climate records from the Summer Lake, Mono Lake, Owens Lake, and Pyramid Lake basins are presented herein. These surface-water systems span 1000 km of latitude and are located near the western margin of the Great Basin, western US (Fig. 1). Today, and in the past, the four surface-water systems receive(d) fluid input mostly derived from cool-season frontal systems associated with the movement of the polar jet stream (PJS) (Pyke, 1972; Manabe and Broccoli, 1985; Kutzbach and Guetter, 1986; Benson and Thompson, 1987). Discovered by Ooishi (1926), the PJS is a permanent feature of the climate system and can be thought of as a teleconnection that links hemispheric weather anomalies along a moderately narrow band. Today, the time-integrated width of the precipitation anomaly spans ~1500 km and is concentrated slightly north of the jet (Starrett, 1949; Riehl et al., 1954).

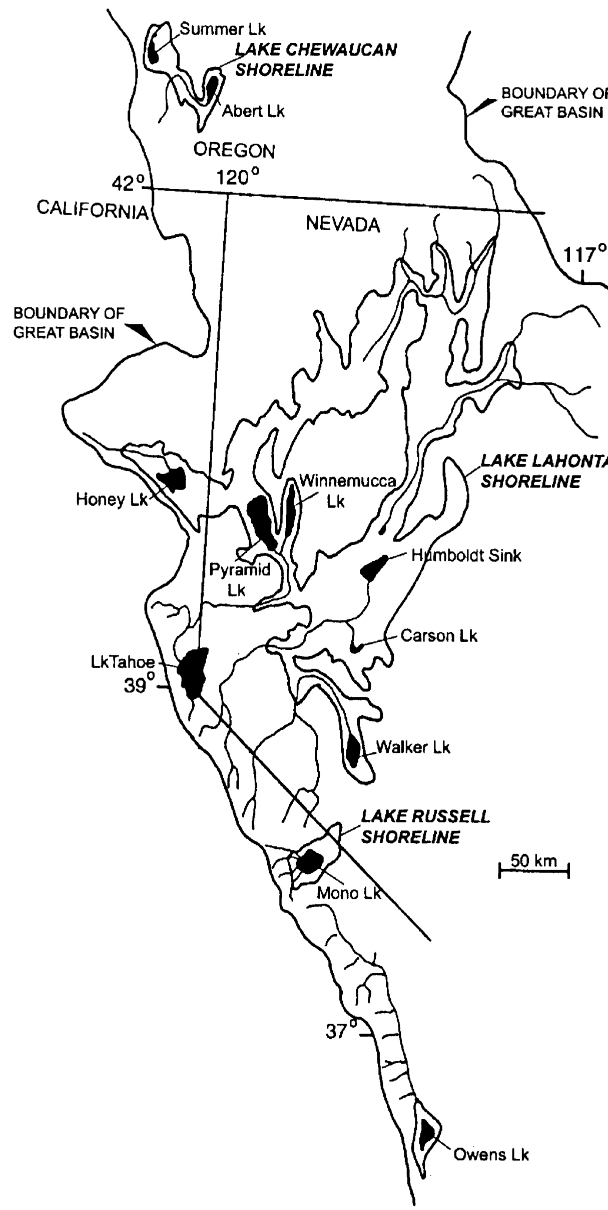


Fig. 1. Map showing locations of principal lakes in the western Great Basin. Solid areas indicate lakes and sinks that held water at least intermittently within the last 100 yr. Also shown are the boundaries of these lake systems during their highstands (between ~16,000 and ~14,000 cal yr B.P.).

During the last late-Pleistocene lake cycle, Summer Lake and Lake Abert coalesced to form Lake Chewaucan, a hydrologically closed system (Russell, 1884). Mono Lake remained hydrologically closed (Russell, 1889), Owens Lake frequently overflowed to China Lake (Smith et al., 1997), and Pyramid Lake (part of Lake Lahontan) overflowed at various times and elevations to three adjacent basins (Russell, 1885). Today, all four basins are hydrologically closed and water diversion has resulted in the desiccations of Summer Lake and Owens Lake.

## 2. Previous high-resolution studies of western Great Basin lakes

High-resolution (sample resolution $<100$ yr), $^{14}$C-based records of Great Basin lakes have previously been published by Benson and his colleagues, including studies of Owens Lake (Benson et al., 1996; Benson et al., 1998a), Mono Lake (Benson et al., 1998b), and Pyramid Lake/Lake Lahontan (e.g., Benson, 1999). These records amply demonstrate that centennial-to-millennial-scale climate change occurred in the western Great Basin during the late Pleistocene; however, age control for these records has not been adequate to demonstrate a clear relationship to D–O cycles (Benson, 1999). One of the issues with regard to correlation is whether large and abrupt oscillations in the air-temperature regime of the North Atlantic or tropical Pacific would be expected to result in near-synchronous changes in the hydrologic balances of Great Basin surface-water systems. It can be argued that atmospheric propagation of a temperature perturbation could instantaneously affect the mass balance of Sierran glaciers inasmuch as summer temperature appears to control the rate of glacier ablation. However, it is not obvious that air temperature by itself can cause a major change in the hydrologic balance of a Great Basin lake. Evaporation from a lake surface does not simply depend on the air temperature of the boundary layer that overlies the lake surface. Instead, it depends on the gradients of temperature and humidity that exist between the lake surface and the boundary layer. If a cooler air mass is advected over a lake basin, the lake's surface layer also cools in response, thereby reducing the temperature gradient and potential evaporation rate.

Late-Pleistocene variability in the hydrologic balances of Great Basin lakes is perhaps best understood in terms of the repositioning of the mean path of the PJS (e.g., Benson and Thompson, 1987). For example, Hostetler and Benson (1990) used a coupled thermal-water balance model to show that the introduction of cloud cover associated with a jet-stream climatology would, by itself, reduce evaporation from Pyramid Lake/Lake Lahontan by $\sim 1/3$rd.

Zic et al. (2002) recently published an isothermal remanent magnetization (IRM) record from Summer Lake, Oregon, that they correlated with the GISP2 record. The IRM record is primarily an indicator of the amount of magnetite in a sample. Zic et al. (2002) have argued that low magnetite values resulted from reductive dissolution of magnetite under anerobic conditions produced by decomposition of organic matter during periods of high productivity. They hypothesized that these conditions occurred during shallow-water stadial periods. This argument is supported by data from other cores taken in the Summer Lake basin that show that low IRM values are associated with high total organic carbon (TOC) values, an indicator of productivity (Negrini et al., 2000). Furthermore, low IRM values were also shown to correspond to low-lake intervals in other cores from the Summer Lake Basin as inferred from lithologic, granulometric, and paleontological proxies for lake size (Cohen et al., 2000; Negrini et al., 2000).

Zic et al. (2002) stretched the IRM record, plotted on a log scale, so as to match positive excursions in IRM (deep-water Summer Lake/Lake Chewaucan interstades) with D–O interstades. The argument for matching Summer Lake/Lake Chewaucan wet periods with Greenland interstades is, on its face, not as strong as the Bond et al. (1993) argument for stretching of North Atlantic marine SST proxy records to match the Greenland $\delta^{18}$O air-temperature proxy record; i.e., SST and air temperature in the North Atlantic should covary. However, Zic et al. (2002) did show that increases in historical (AD 1895–1984) precipitation falling in the Summer Lake region correlated with increases in Greenland air temperatures (increases in $\delta^{18}$O).

Given the intriguing correlation of Zic et al. (2002), we performed $\delta^{18}$O analyses of the unaltered ostracode fraction from samples of their B&B core. $\delta^{18}$O has been previously shown to be an indicator of change in the hydrologic balance of other Great Basin lakes on monthly, decadal, centennial, and millennial scales (Benson et al., 1998b; Benson, 1999; Benson and Paillet, 2002; Benson et al., 2003b).

## 3. Age models for Great Basin Lake records

One of the objectives of this paper is to employ linked age models for Great Basin climate records that are independent of, rather than stretched to match, the GISP2 record. We used climate records from four lake basins: Summer, Pyramid, Mono, and Owens (Fig. 1). Pyramid Lake core PLC92B and Owens Lake core OL90-2 have the most complete and consistent $^{14}$C data sets. In addition, Pyramid Lake exhibited only a small ($\leqslant 600$ yr) reservoir effect during the late Holocene (Benson et al., 2002). Our overall strategy was to transfer parts of the PLC92B $^{14}$C record to other sediment records, using the PLC92B-based ages of two well-dated tephra (Wono tephra and Wilson Creek Ash #15)(Fig. 2).

All four climate records were linked to core PLC92B via the position of Ash #15 or via distinctive paleomagnetic features in the Mono Lake excursion (MLE) associated with Ash #15. This tephra occurs within the upper part of the lower of two magnetic inclination peaks associated with the MLE (see Fig. 10b in Liddicoat, 1992). For records that contain the MLE, but do not contain Ash #15, we refer to the location of

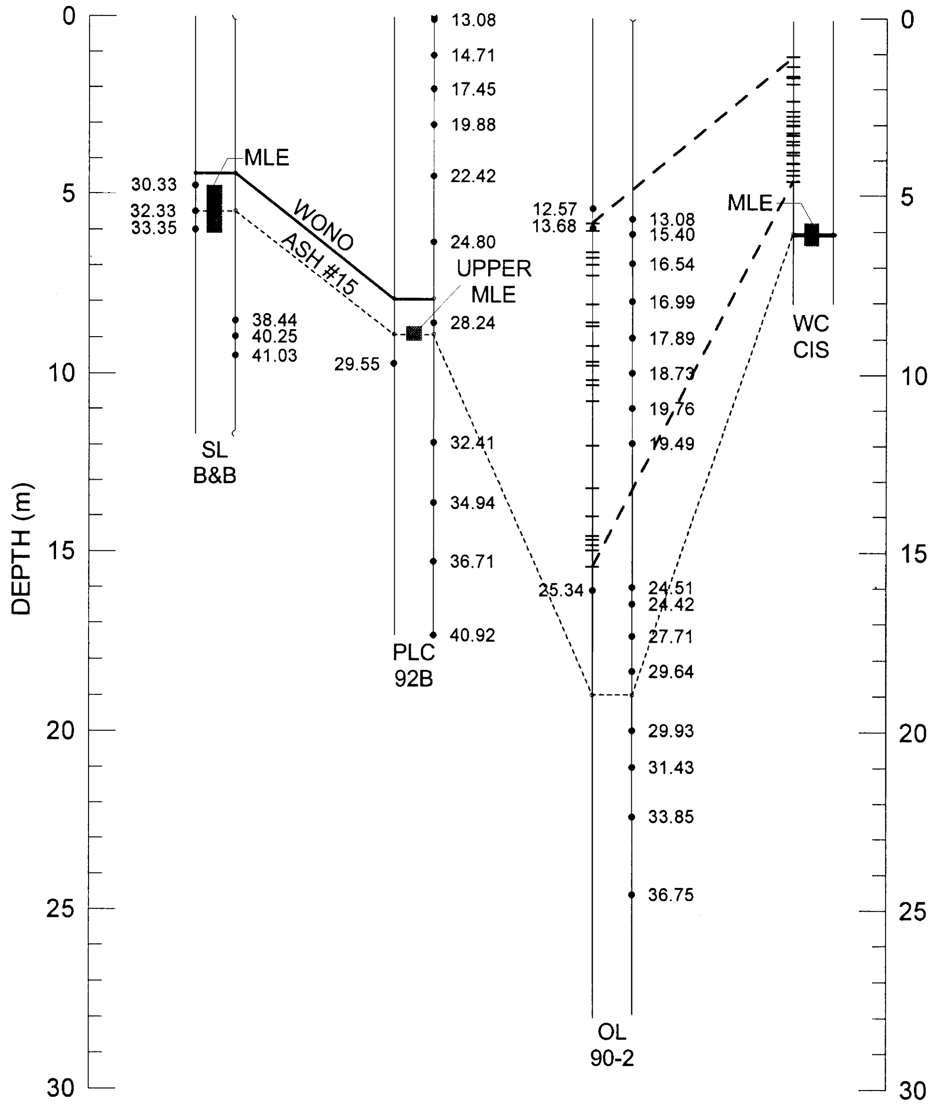


Fig. 2. Plot showing raw $^{14}C$ age control and tie points between the Summer Lake B&B core, Pyramid Lake core PLC92B, Owens Lake core OL90-2, and the WC CIS. Locations of $^{14}C$ dates are shown by small filled circles; dates are listed as $10^3$ yr B.P. The heavy dashed lines drawn between OL90-2 and the WC CIS connect the upper and lower values of a series of PSV tie points shown as thin dashes on the left sides of the cores. The location of the MLE is shown by a solid rectangle. The entire MLE is present in SL B&B and in the WC CIS; only the upper part of the MLE is found in the Pyramid Lake basin. The dotted line connects the actual location of Ash #15 or the paleomagnetic feature associated with MLE15 in all four basins. Ash #15 is present within the MLE in the WIC CIS. The position of MLE15 in PLC92B was determined using its position relative to the positions of well-dated tephras found in sites that border Pyramid Lake (Benson et al., 2003a). MLE15 in the SL B&B core was determined from its position within the MLE. MLE15 in OL90-2 was obtained from extrapolation of a PSV-based correlation between OL90-2 and the WC CIS (Fig. 3D).

the distinctive paleomagnetic feature that is elsewhere associated with Ash #15 as the MLE15 feature.

Comparison of the PLC92B $^{14}C$-based age of Ash #15 with its estimated $^{14}C$ age in other lake records allows us to estimate the reservoir effect in each of the other lakes. For the calculation, the Pyramid Lake reservoir effect was assumed negligible. This assumption is an approximation and derives from the fact that Pyramid Lake may have been hydrologically closed during much of the late Holocene; however, between 45,500 and 23,000 yr B.P. the lake frequently overflowed into either the Winnemucca Lake Basin or the Smoke-Creek Desert. During overflow, the dissolved inorganic carbon (DIC) concentration rapidly decreases, facilitating the $CO_2$ exchange process, thus reducing the magnitude of the reservoir effect.

Reservoir-corrected $^{14}C$ data were then used to construct calendar-age models for each of the lake records, using the calibration data set of Voelker et al. (1998). Because this particular calibration is tied to the GISP2 age model, corresponding calibrated ages should be closely equivalent to GISP2 ages.

### 3.1. The Pyramid Lake (Lake Lahontan) age model

The age model for core PLC92B is based on 12 AMS $^{14}C$ values (Table 1). Pyramid Lake was assumed to have a zero reservoir effect, and the raw $^{14}C$ values were converted to GISP2 ages (Fig. 3A) using the Voelker et al. (1998) data set (See Fig. 2 in Benson et al., 2003a). Because the assumption of zero reservoir effect is an approximation, the reader may wish, when viewing the lake-based climate records, to visually "slide" the records by as much as 600 yr in the "younger" direction.

### 3.2. The Summer Lake B&B age model

The age model for the B&B core was linked to core PLC92B via the positions of the Wono tephra and Ash #15 in PLC92B and the position of the Wono Tephra and MLE15 in the B&B core (Fig. 2). The value of the Summer Lake reservoir effect (~3500 yr) was obtained by subtracting the $^{14}C$ age of MLE15, obtained from a linear fit to the raw $^{14}C$ data for the B&B core (Table 1), from the $^{14}C$ age of Ash #15 (28,620 ± 300 $^{14}C$ yr B.P.), obtained from the PLC92B $^{14}C$ age model (Benson et al., 2003a). The reservoir effect was then subtracted from the raw B&B $^{14}C$ data (Table 1) (Fig. 3B) and the reservoir-corrected $^{14}C$ data were converted to GISP2 ages (Fig. 3C).

### 3.3. The Owens Lake age model

The OL90-2 age model was created by correlating 27 distinctive inclination and declination features found in the upper parts of the Wilson Creek composite isotope section (WC CIS) and core OL90-2 (Figs. 2, 4, Table 2). The depth–depth relation resulting from this correlation was extrapolated to the MLE15 feature in core OL90-2 (Fig. 3D). The age of Ash #15, estimated from the PLC92B age model, was compared with the apparent age of MLE15 in the OL90-2 record which had been calculated using a raw $^{14}C$ age model, developed from the OL90-2 $^{14}C$ data set (Table 2). It was determined that a reservoir effect of ~450 yr existed in Owens Lake at the time of MLE15. The reservoir effect was subtracted from the raw OL90-2 $^{14}C$ data (Table 1) and the reservoir-corrected $^{14}C$ data were converted to GISP2 ages (Fig. 3E).

### 3.4. The Mono Lake/Wilson Creek Formation age model

The Wilson Creek Formation contains 19 volcanic tephra (ashes) which form the basis of stratigraphic control in the basin. The interval between Ash 4 and 5 is contorted and deformed in the Wilson Creek type section. To rectify this problem, samples that spanned this interval were obtained from the Wilson Creek South Shore site for use in constructing both the WC CIS (Benson et al., 1998b) and the Wilson Creek composite paleomagnetic section (WC CPS) (Lund et al., 1988). In this paper, all isotopic and age data from the Wilson Creek Formation are given relative to depths in the WC

Table 1
Depth, $^{14}C$, and GISP2 ages of samples from cores PLC92B, OL90-2, and SL B&B

| CAMS# | Depth (m) | $^{14}C$ age $10^3$ yr B.P. | ± $10^3$ yr B.P. | GISP2 age $10^3$ yr |
|---|---|---|---|---|
| Core PLC92B | | | | |
| 10638 | 0.075 | 13.08 | 0.06 | 15.16 |
| 10781 | 1.075 | 14.71 | 0.07 | 16.86 |
| 10782 | 2.025 | 17.45 | 0.10 | 19.84 |
| 10783 | 3.025 | 19.88 | 0.13 | 22.57 |
| 10639 | 4.475 | 22.42 | 0.11 | 25.47 |
| 10663 | 6.325 | 24.80 | 0.15 | 28.18 |
| 10640 | 8.575 | 28.24 | 0.19 | 32.02 |
| 10641 | 9.675 | 29.55 | 0.23 | 33.44 |
| 10784 | 11.925 | 32.41 | 0.42 | 36.40 |
| 10643 | 13.625 | 34.94 | 0.47 | 38.82 |
| 10644 | 15.275 | 36.71 | 0.50 | 40.38 |
| 10655 | 17.325 | 40.92 | 0.96 | 43.54 |
| Core SL B&B | | | | |
| 84217 | 4.76 | 30.33 | 0.29 | 30.49 |
| 88145 | 5.50 | 32.33 | 0.64 | 32.69 |
| 9253 | 6.00 | 33.35 | 0.40 | 33.78 |
| 15022 | 8.52 | 38.44 | 1.06 | 38.84 |
| 15023 | 8.96 | 40.25 | 1.29 | 40.43 |
| 15024 | 9.50 | 41.03 | 1.43 | 41.07 |
| 9254 | 11.38 | 37.61 | 0.69 | |
| Core OL90-2 | | | | |
| 13469 | 5.370 | 12.57 | 0.08 | 14.19 |
| 13527 | 5.670 | 13.08 | 0.06 | 14.70 |
| 13470 | 5.940 | 13.68 | 0.07 | 15.31 |
| 13471 | 6.090 | 15.40 | 0.11 | 17.12 |
| 13528 | 6.920 | 16.54 | 0.18 | 18.35 |
| 13529 | 7.970 | 16.99 | 0.19 | 18.84 |
| 13472 | 8.980 | 17.89 | 0.20 | 19.83 |
| 13524 | 9.960 | 18.73 | 0.39 | 20.77 |
| 13526 | 10.950 | 19.76 | 0.36 | 21.93 |
| 13473 | 11.940 | 19.49 | 0.27 | 21.62 |
| 13475 | 15.990 | 24.51 | 0.18 | 27.34 |
| 20221 | 16.090 | 25.34 | 0.35 | 28.29 |
| 21537 | 16.450 | 24.42 | 0.20 | 27.24 |
| 21542 | 17.340 | 27.71 | 0.25 | 30.95 |
| 20222 | 18.320 | 29.64 | 0.36 | 33.05 |
| 20223 | 19.960 | 29.93 | 0.35 | 33.36 |
| 20224 | 20.990 | 31.43 | 0.44 | 34.94 |
| 20225 | 22.375 | 33.85 | 0.60 | 37.37 |
| 20226 | 24.565 | 36.75 | 0.81 | 40.03 |

GISP2 ages calculated from Voelker et al. (1998); see Fig. 2 in Benson et al. (2003a). OL90-2 raw $^{14}C$ ages were corrected for a reservoir effect of 450 yr before conversion to GISP2 yr. Summer Lake B&B ages were corrected for a reservoir effect of 3500 yr before conversion to GISP2 yr. CAMS# 9254 was not used in the B&B age model as the date was stratigraphically out of order. CAMS is the Center for Accelerator Mass Spectrometry at Lawrence Livermore National Laboratory.

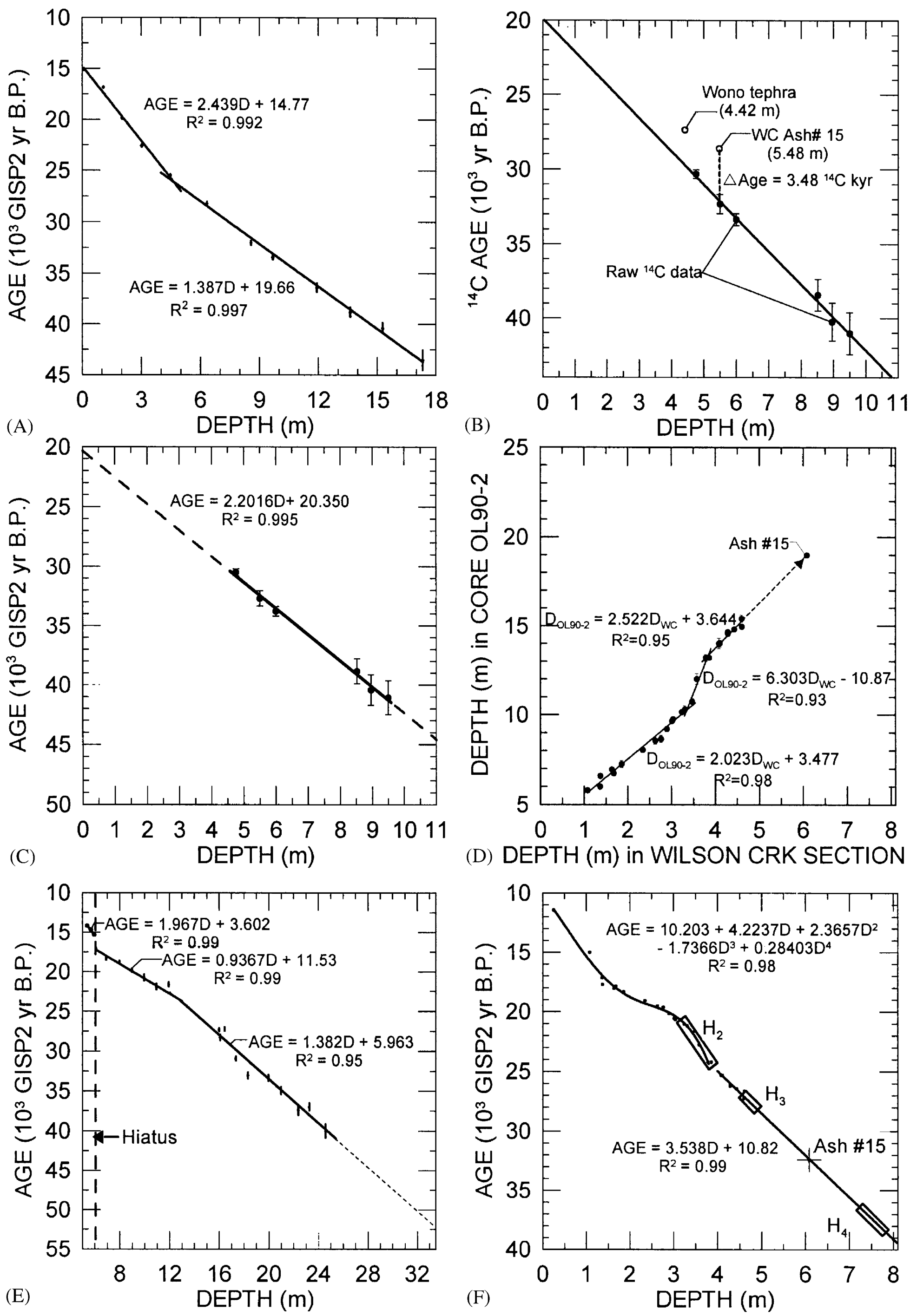


Fig. 3. Age models for Pyramid, Summer, Owens and Mono lake systems. Radiocarbon years have been converted to GISP2 yr using the data of Voelker et al. (1998). (A) Age model for Pyramid Lake core PLC92B based on $^{14}$C data published in Benson et al. (1997) (Table 1). (B) Raw $^{14}$C date for Summer Lake B&B core (solid circles). Open circles indicate ages of Wono tephra and MLE15 calculated from their positions in core PLC92B. The position of MLE15 in the B&B core was calculated from its position within the MLE in the WC CPS (Lund et al., 1988) and the location and shape of the MLE within the B&B core (Negrini et al., 2000). Δage refers to the value of the reservoir effect in Summer Lake at the time of the deposition of Ash #15 in the Pyramid Lake basin (28,620±300 $^{14}$C yr B.P.; Benson et al., 2003a). (C) Age model (GISP2 yr) for the B&B core was constructed using the raw $^{14}$C data (Fig. 3B) corrected for a 3500 yr reservoir effect and the data of Voelker et al. (1998). Note that good age control for the B&B core extends from only ~41,000 to 30,000 GISP2 yr (thick solid line). (D) Depth–depth correlation between magnetic features in the WC CIS and Owens Lake core OL90-2 (Table 2). An extrapolation to MLE15 in core OL90-2 is shown. Note that the correlation extends only from 1.1 to 4.7 m (~27,000 GISP2 yr) in the Wilson Creek section. (E) Age model (GISP2 yr) for core OL90-2 based on $^{14}$C data presented in Benson et al. (1996) (Table 1). (F) Age model for the WC CIS based on paleomagnetic feature correlations between the WC CIS (Lund et al., 1988) and core OL90-2 (Fig. 2, Table 2) and the core OL90-2 age model (Fig. 3E). The open rectangles indicate the hypothetical locations of Heinrich events 2, 3, and 4, in the WC CIS based on a match of paleomagnetic features in the WC CIS and in north Atlantic sediment cores (Table 3) (Benson et al., 1998a, b). Dates for the Heinrich events were taken from the GISP2 core (Grootes and Stuiver, 1997).

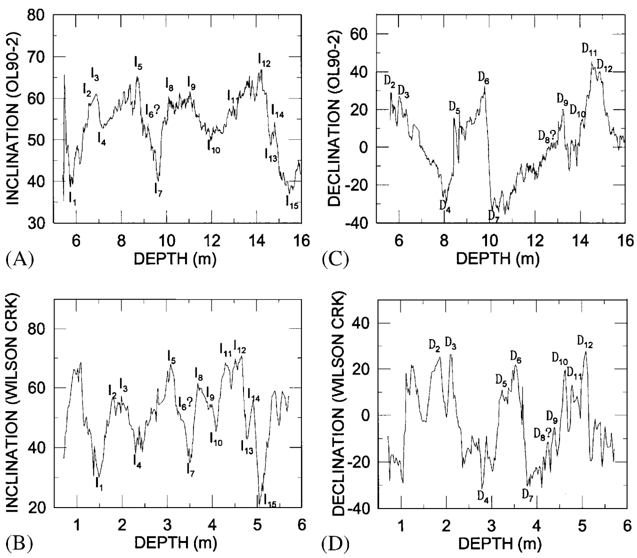


Fig. 4. Correlation of paleomagnetic features in core OL90-2 and the WC CPS. Inclination features in core OL90-2 (A) and the Wilson Creek (B) section. Declination features in core OL90-2 (C) and the Wilson Creek (D) section.

Table 2
Depth (m) of tephra and paleomagnetic features in Wilson Creek (WC) composite paleomagnetic section (CPS), Wilson Creek (WC) composite isotope section (CIS), and Owens Lake (OL) core OL90-2

| Feature | Depth WC CPS (m) | ± (m) | Depth WC CIS (m) | ± (m) | Depth OL (m) | ± (m) |
|---|---|---|---|---|---|---|
| ASH#3 | 0.63 | | 0.25 | | | |
| I1 | 1.49 | 0.05 | 1.68 | 0.05 | 5.80 | 0.15 |
| D2 | 1.79 | 0.05 | 1.97 | 0.05 | 6.00 | 0.05 |
| I2 | 1.80 | 0.02 | 1.98 | 0.02 | 6.60 | 0.10 |
| I3 | 2.07 | 0.05 | 2.24 | 0.05 | 6.95 | 0.10 |
| D3 | 2.12 | 0.02 | 2.29 | 0.02 | 6.75 | 0.15 |
| I4 | 2.30 | 0.02 | 2.46 | 0.02 | 7.25 | 0.20 |
| D4 | 2.81 | 0.02 | 2.95 | 0.02 | 8.05 | 0.15 |
| I5 | 3.10 | 0.05 | 3.24 | 0.05 | 8.55 | 0.20 |
| D5 | 3.24 | 0.02 | 3.37 | 0.02 | 8.65 | 0.20 |
| I6 | 3.38 | 0.02 | 3.50 | 0.02 | 9.20 | 0.10 |
| I7 | 3.50 | 0.02 | 3.62 | 0.02 | 9.65 | 0.10 |
| D6 | 3.53 | 0.05 | 3.64 | 0.05 | 9.75 | 0.10 |
| I8 | 3.74 | 0.05 | 3.85 | 0.05 | 10.15 | 0.10 |
| D7 | 3.81 | 0.02 | 3.91 | 0.02 | 10.30 | 0.20 |
| I9 | 3.98 | 0.02 | 4.08 | 0.02 | 10.75 | 0.15 |
| I10 | 4.09 | 0.02 | 4.18 | 0.02 | 12.00 | 0.30 |
| I11 | 4.30 | 0.02 | 4.39 | 0.02 | 13.20 | 0.20 |
| D9 | 4.38 | 0.02 | 4.47 | 0.02 | 13.20 | 0.10 |
| ASH#5 | 4.41 | | 3.89 | | | |
| ASH#6 | 4.50 | | 4.02 | | | |
| ASH#7 | 4.57 | | 4.06 | | | |
| D10 | 4.61 | 0.02 | 4.28 | 0.02 | 14.00 | 0.20 |
| I12 | 4.59 | 0.05 | 4.25 | 0.05 | 14.00 | 0.30 |
| D11 | 4.78 | 0.02 | 4.46 | 0.02 | 14.55 | 0.10 |
| I13 | 4.78 | 0.02 | 4.46 | 0.02 | 14.65 | 0.10 |
| I14 | 4.92 | 0.02 | 4.60 | 0.02 | 14.80 | 0.10 |
| D12 | 5.08 | 0.05 | 4.78 | 0.05 | 14.95 | 0.10 |
| I15 | 5.07 | 0.05 | 4.77 | 0.05 | 15.40 | 0.20 |
| ASH#8 | 5.72 | | 5.30 | | | |

CIS (Table 2). To convert from depth in the WC CPS to depth in the WC CIS, the location of a feature relative to its position between bracketing ash layers was considered constant. Part of the core OL90-2 age model (Fig. 3E) was linked to the WC CIS by matching paleomagnetic features (Fig. 2). The WC CIS age model is based on this linkage (dots connected by fourth-order polynomial in Fig. 3F) and a linear extrapolation from the oldest paleomagnetic tie point through the position and age of Ash #15 to the base of the WC CIS (Fig. 3F). The locations of Heinrich events ($H_2$, $H_3$, and $H_4$) in the WC CIS, as determined by Benson et al., 1998b, were plotted on the WC CIS age model (open rectangles in Fig. 3F). A comparison of the age ranges for each of the events with the midpoint of its age range deduced from its position in the GISP2 ice core (Table 3) indicates that the WC CIS age model yield dates that are ~1300 yr too young at the time of Heinrich event 4; i.e., at ~38,800 GISP2 yr B.P.

### *3.5. Relative values of the reservoir effect*

Above, we showed that reservoir effects for Pyramid Lake and Owens Lake were small compared to those for Mono and Summer lakes. We suggest that the value of the reservoir effect was largely due to the hydrologic state of each lake. Pyramid and Owens lakes were often hydrologically open during the late Pleistocene, whereas Mono and Summer lakes remained closed. DIC and calcium (Ca) are mainly introduced to Great Basin lakes via river discharge. In general, input waters have DIC/Ca ratios $>1$; therefore, as $CaCO_3$ precipitates from lake water, the concentration of DIC increases monotonically with time. During hydrologic closure, the increase of DIC over time makes gas exchange less efficient and the value of the reservoir effect increases. There are two ways in which the surplus DIC (the source of the reservoir effect) can be removed from a lake: overflow and gas exchange. The residence time, and hence concentration of the DIC, in an overflowing lake is inversely proportional to the rate of overflow. Thus the faster the rate of overflow, the greater the efficiency of exchange of modern atmospheric carbon for "dead" lake carbon.

## 4. Methods used in obtaining $\delta^{18}O$ data for the Summer Lake B&B core

Ostracodes (*Limnocythere ceriotuberosa*) were picked from 345 sediment samples taken from the Summer Lake core. Two hundred and sixty sets of ostracodes free from surface contamination were analyzed for $\delta^{18}O$. Powdered carbonate material was analyzed using a Micromass Optima gas-source triple-collector mass spectrometer equipped with a dual inlet and interfaced

Table 3
Depths and estimated GISP2 ages of Heinrich events in the Wilson Creek composite isotope section (WC CIS) and the GISP2 ice core

| Event | Depth (m) | $GISP2_V$ age $10^3$ yr B.P. | $GISP2_{IC}$ age $10^3$ yr B.P. | Age difference $10^3$ yr B.P. |
|---|---|---|---|---|
| H2 (top) WC CIS | 3.18 | 20.78 | | |
| H2 in GISP2 | | | 24.0 | −1.3 |
| H2 (bottom) WCS | 3.88 | 24.55 | | |
| H3 (top) WC CIS | 4.57 | 26.99 | | |
| H3 in GISP2 | | | 29.8 | −2.2 |
| H3 (bottom) WC CIS | 4.90 | 28.16 | | |
| H4 (top) WC CIS | 7.23 | 36.40 | | |
| H4 in GISP2 | | | 38.8 | −1.3 |
| H4 (bottom) WC CIS | 7.83 | 38.52 | | |

$GISP2_V$ age indicates that data from Voelker et al. (1998) were used to estimate the age of the event in the Wilson Creek section and $GISP2_{IC}$ indicates that the age was estimated from the position of the midpoint of the Heinrich event in the ice core. Age difference indicates the probable error in the WC CIS age model relative to its GISP2 ice core age.

with a MultiPrep automated sample preparation device. The precision of analyses of reference standard NBS-19 is estimated to be $\pm 0.04‰$ for $\delta^{18}O$. About 20 mg of clean ostracodes were taken from depths of 4.76 and 5.50 m in the B&B core and analyzed for $^{14}C$ at the CAMS facility at the Lawrence Livermore National Laboratory (Table 1).

## 5. Proxies of climate change

### 5.1. Total organic carbon (TOC) records (Fig. 5, columns 2 and 3)

Benson et al. (1996, 1998a) have shown that the Owens Lake TOC record reflects changes in water temperature and the amount of sediment delivered to Owens Lake during stadial and interstadial events. During glacial stades, glacial rock flour was input to the Owens basin surface-water system. The turbid water decreased light penetration and photosynthetic productivity, reducing the amount of TOC produced within the lake. Seasonal ice cover and decreased water temperatures associated with glacial stades led to further decreases in productivity. In addition, the increased glacial clastic flux diluted the fraction of organic carbon deposited in lake sediment.

### 5.2. Total inorganic carbon (TIC) records (Fig. 5, column 4)

Oscillations in TIC have been shown to correlate well with oscillations in $\delta^{18}O$ on a variety of time scales in Great Basin lakes (e.g., Benson et al., 2003b). The mass of calcium input to most Great Basin lakes is a linear function of discharge, whereas the mass of siliciclastic sediment is an exponential function of discharge. This implies that the fraction of TIC deposited in the sediments of a hydrologically closed lake should decrease with increasing discharge (increasing lake size) and vice versa (Benson et al., 2002). When a lake overflows, a further reduction in the fraction of TIC occurs because much of the inorganic carbon reaching the lake is lost via overflow.

### 5.3. The GISP2 $\delta^{18}O$ record (Fig. 5, column 1)

The GISP2 $\delta^{18}O$ record is primarily a record of air temperature (Jouzel et al., 1997), with more negative values of $\delta^{18}O$ indicating times of decreased temperatures (stades). In the past few years, studies involving nitrogen and argon isotopes, contained in air trapped in polar ice cores, have shown that Greenland surface temperatures rose rapidly at the beginning of interstadials; i.e., $16 \pm 2°C$ at the beginning of D–O interstade 19 (Lang et al., 1999), $15 \pm 3°C$ at the beginning of the Younger Dryas event (Severinghaus et al., 1998), and $\sim 16°C$ for the Bølling transition (Fig. 2 in Severinghaus and Brook, 1999).

### 5.4. Lacustrine $\delta^{18}O$ records (Fig. 5, columns 5 and 6)

The $\delta^{18}O$ records of Great Basin lakes primarily reflect changes in lake volume (see Appendix A in Benson and Paillet, 2002), with a decrease in $\delta^{18}O$ indicating an increase in lake volume or an increase in the rate of overflow. Some part of the variability in $\delta^{18}O$ is associated with changes in air and water temperature; however, the amount of variability associated with temperature change is difficult to evaluate quantitatively. For example, if it is assumed that stadial cooling of the Sierra Nevada was $\sim 5°C$, the change in snowpack $\delta^{18}O$ would be –3.5‰, for the elevations over which snow accumulates today (calculation assumes that $d\delta^{18}O/dT_{AIR} = 0.7‰\,°C^{-1}$; Dansgaard, 1964). However, changes in surface-water temperature tend to parallel changes in air temperature (e.g., see Table 5 in Benson and Paillet, 2002). Therefore, the $\delta^{18}O$ values of $CaCO_3$ precipitated from the same $\delta^{18}O$ value of lake water, but at the colder water temperature,

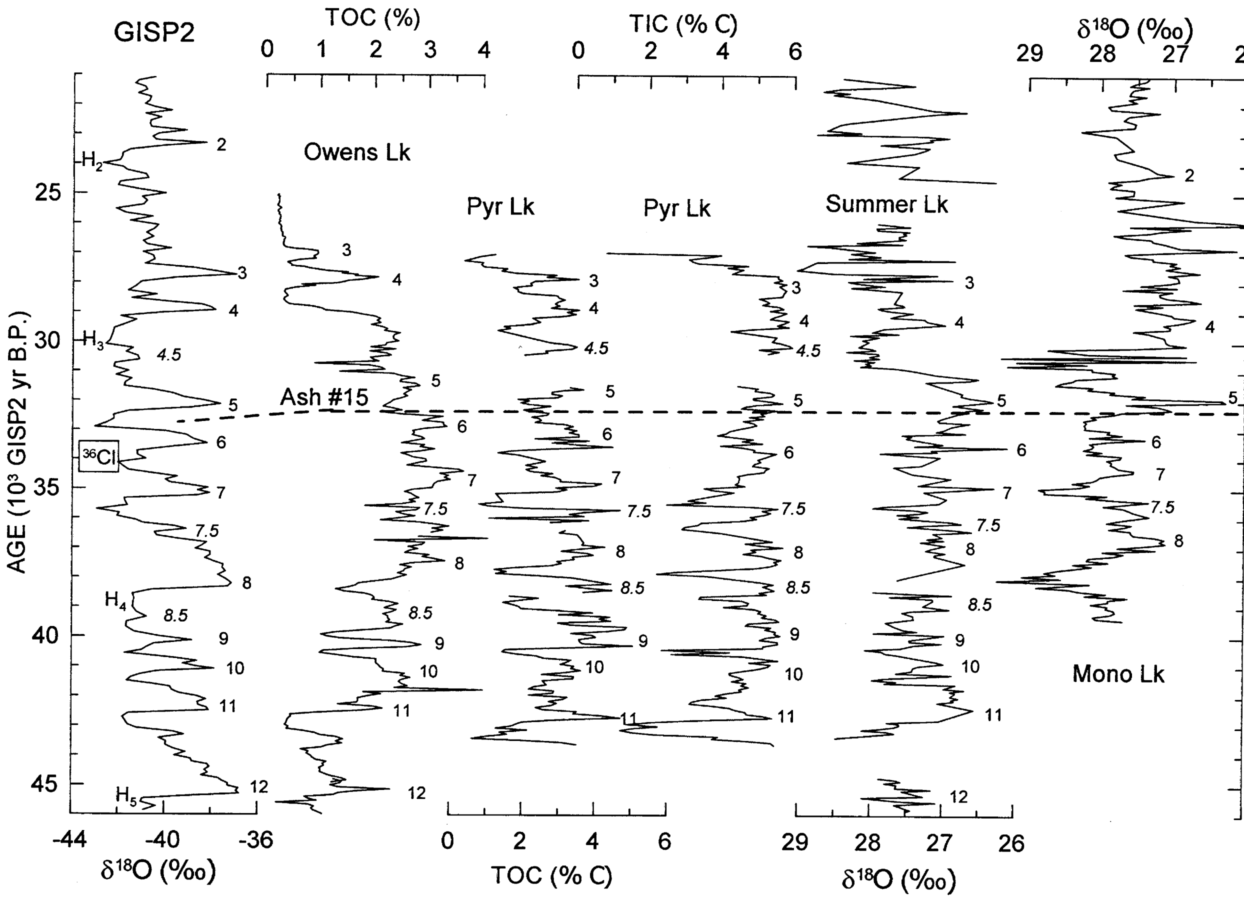


Fig. 5. Great Basin lake TOC, TIC, and $\delta^{18}O$ records compared with the GISP2 $\delta^{18}O$ record between 46,000 and 21,000 GISP2 yr. Age models for these records are shown in Fig. 3. D–O interstades are numbered (2–12) and Heinrich events are denoted by a capital H with the event number in subscripts ($H_2$–$H_5$). We have applied an informal D–O designation of 4.5, 7.5 and 8.5 to three minor peaks within the GISP2 record that also appear within the Summer, Pyramid, and Owens lake records. The location of Ash #15 or MLE15 is indicated by the dashed horizontal line. Ash #15 is located above the paleomagnetic low-intensity region of the MLE (Liddicoat, 1992). The low-intensity region is roughly equivalent in time to a $^{36}Cl$ anomaly observed in the GISP2 core between D–O events 6 and 7 (Wagner et al., 2000).

would be ~1.1‰ heavier (assumes that $d\delta^{18}O/dT_{WATER} = 0.22‰\,°C^{-1}$; O'Neil et al., 1969). The net −2.4‰ change in the $\delta^{18}O_{CaCO3}$ record represents a maximum negative value because stadial precipitation probably occurred at lower (warmer) elevations than it does today and also because cold-air drainage from Sierran alpine glaciers would have further lowered the surface-water temperatures of lakes located downslope from ice fields. Because the effect of a temperature decrease on the $\delta^{18}O$ value of a carbonate precipitated during a cold period is to decrease the value, the degree of wetness during a cold period is overestimated by its $\delta^{18}O$ value.

## 6. Linking lacustrine and GISP2 records

The position of MLE15 was linked to the GISP2 $\delta^{18}O$ record (Fig. 5, column 1) using the following procedure. A record of relative paleomagnetic field intensity for the North Atlantic region has been constructed by integrating magnetic data from six marine sediment cores (NAPIS-75 stack). The stacked record was linked to the GISP2 age model by correlation of the marine planktonic $\delta^{18}O$ record to the GISP2 ice-core $\delta^{18}O$ record (Laj et al., 2000). An intensity low centered at ~34,500 GISP2 yr B.P. in the NAPIS-75 stack identified by Laj et al. (2000) as the MLE has also been linked to a distinct perturbation in the $^{36}Cl$ flux rate between D–O events 6 and 7 (32,800 and 34,500 GISP2 yr B.P.) in the GRIP ice core (Wagner et al., 2000). The peak in the $^{36}Cl$ flux rate can be attributed to a minimum of the geomagnetic dipole field associated with the MLE. The MLE15 signature occurs above this intensity minimum and is located between D–O events 5 and 6 in Great Basin lakes.

## 7. Results

For the most part, the Owens Lake and Pyramid Lake TOC alpine-glacial proxy record (Fig. 5, columns 2, 3) bear a remarkable resemblance to the GISP2 $\delta^{18}O$

record with maxima in the TOC records (Sierran interstades) corresponding to D–O interstades. This is consistent with the hypothesis that D–O stades are associated with a lowering of temperature across the Northern Hemisphere and vice versa. However, because we have not provided multiple linkages between the GISP2 and lacustrine records, we cannot assert unequivocally that Sierran glacial stades were synchronous with D–O stades.

The Summer Lake and Mono Lake $\delta^{18}O$ records (Fig. 5, columns 5 and 6) have been linked using the position of Ash #15 or the MLE15 feature. The $\delta^{18}O$ records for the two lakes indicate wet periods on either side of Ash #15 which we associate with D–O interstades 5 and 6. We also correlate other wet events in the $\delta^{18}O$ records with D–O interstades 2–12, noting that Heinrich events $H_3$ and $H_4$ appear to have been associated with relatively dry intervals. The correlation in time (anti-phasing) between the Summer Lake and GISP2 $\delta^{18}O$ records is quite good. However, the correlations become more hypothetical with time/distance away from the MLE15 tie line. For example, the Mono Lake and GISP2 $\delta^{18}O$ records are out of phase by about 1500 yr at the time of D–O interstade 8 (Fig. 5). This is consistent with inaccuracies in the Mono Lake age model that were discussed in Section 3.4.

A comparison of the Summer Lake $\delta^{18}O$ record with the Owens Lake TOC record suggests that $\delta^{18}O$ minima (wet periods) were associated with TOC maxima (warm periods). This correlation is weak because the MLE15 feature is the only link between the two records. The best way to determine the relative phasing of glacial and hydrologic oscillations is to compare proxy records from a single sediment core. TOC and $\delta^{18}O$ records both exist for Owens Lake and Pyramid Lake (Benson, 1999 and references therein); however, after 37,500 GISP2 yr B.P., high rates of overflow in both basins, together with decreased water temperatures, allowed only intermittent precipitation of $CaCO_3$. Precipitation probably occurred most frequently during warm, low-overflow periods. Therefore, the $\delta^{18}O$ records are not representative of typical or even average overflow conditions (Benson et al., 1996).

However, maxima in TIC records have been shown to correlate extremely well with maxima in $\delta^{18}O$ records over a variety of time scales (e.g., Benson et al., 2002, 2003b). Thus we can compare TOC variability with TIC variability for the period 43,500–27,000 GISP2 yr B.P. in the Pyramid Lake core (Fig. 5, columns 3 and 4). Such a comparison demonstrates that most Sierran glacial stades were associated with "relatively" dry conditions (TIC maxima).

The Owens Lake record between 51,000 and 37,500 GISP2 yr B.P. allows direct comparison of TOC, the air-temperature proxy, and $\delta^{18}O$, the other hydrologic-balance proxy (Fig. 6). The comparison indicates that

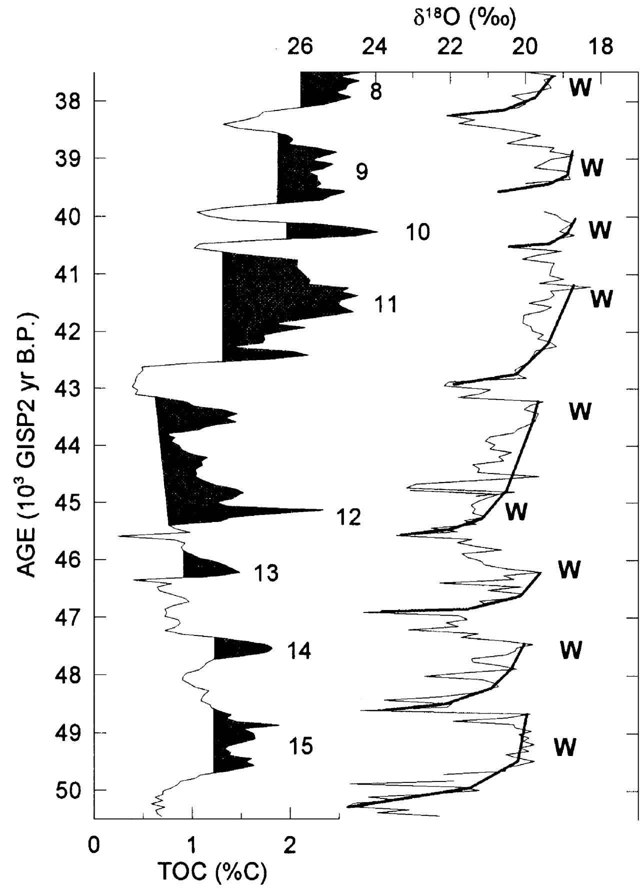


Fig. 6. TOC and $\delta^{18}O$ records for Owens Lake core OL90-1 for the period 51,000–37,500 GISP2 yr B.P. Alpine interstades are numbered and indicated by solid areas with high TOC values. Wet periods (W) are indicated by increases in the negative derivative of $\delta^{18}O$. The heavy segmented lines indicate times of positive changes in the hydrologic balance of Owens Lake.

minima in TOC are generally coincident with maxima in $\delta^{18}O$, suggesting that Sierran stades were characterized by "relatively" dry conditions prior to 37,500 GISP2 yr B.P. (Fig. 6). Decreases in $\delta^{18}O$ were often initiated before increases in TOC, indicating that increases in wetness sometimes preceded the initiation of warming. The association of relatively dry conditions with decreased temperatures is consistent with decrease in saturation vapor pressure as a function of decreasing temperature; i.e., saturated air contains ~28% less moisture for each 5°C decrease in temperature.

It can be argued that coastal California lies upwind from some of the southern Great Basin drainage areas (e.g., Owens Lake) and that similarities in climate records from both areas might be expected. Hendy and Kennett (1999) used $\delta^{18}O$ values from planktonic foraminifera to show that SST was 4–8°C warmer in the Santa Barbara Basin (core ODP 893A located at ~34°N) during interstades. Their data also indicate an absence of vertical water-mass structure during stades which contrasts with evidence for a well-developed thermocline during interstades. In addition, Hendy and Kennett (1999) argue that brief negative excursions in SST ($\sim 3^\circ$C) at the beginning of some interstades were caused by top-down warming of the uppermost surface waters. The additional 4–8°C warming was argued to be caused by replacement of the cool California Current waters with waters of the warm subtropical countercurrent. Their correlation of isotopically light warm events with D–O stades is consistent with our interpretation of TOC maxima with D–O stades (Fig. 5). However, their record has not been linked to the GISP2 record using paleomagnetic secular variation (PSV).

Heusser (1998) analyzed pollen from the same core studied by Hendy and Kennett (1999) and showed that some interstadial events were accompanied by increases in plants that prefer a warm and relatively dry climate (e.g., oak). Heusser (1998) demonstrated that the relative percentage of oak pollen is high during times when Santa Barbara basin sediments are laminated (anaerobic conditions) and when vertical water-mass structures are in place. The pollen data thus appear to indicate that warm and relatively dry conditions persisted along the California coast during some interstades, whereas cold and relatively wet conditions (signaled by peaks in pine and juniper pollen) persisted during some stades. Heusser's (1998) results seem to contradict our association of relatively dry conditions in the Sierra Nevada with stadial conditions. However, it may be that colder temperature, not increased precipitation, was sufficient to cause the replacement of oak by pine along the California coast during stadial events, and that colder ocean temperatures increased the frequency and amount of coastal fog which also encouraged the spread of pine and juniper. In any case, the climate of coastal California can be argued to have little to do with the climate of the Sierra Nevada; in which case, the data sets indicate synoptic variability in climate response of the two regions.

## 8. Summary and conclusions

We have linked four Great Basin lake records of change in hydrologic and/or cryologic balances using paleomagnetic features and locations of tephra whose times of deposition in the Pyramid Lake basin are well known. We have corrected the $^{14}$C records for Mono, Summer, and Owens Lake for reservoir effect by comparing the $^{14}$C age of Ash#15 or the MLE15 feature in these lakes with the $^{14}$C age of the Ash#15 in the Pyramid Lake basin and assuming that the reservoir effect has remained unchanged over the time frame of interest. In addition, we have tied the lake records to the GISP2 $\delta^{18}$O record using a correlation between the MLE/Ash#15 in the lake records and the location of a $^{36}$Cl anomaly/intensity low associated with the MLE in the ice-core record. Reservoir-corrected $^{14}$C data for lake sediments were then used to construct GISP2-equivalent age models for each of the lake records, using the calibration data set of Voelker et al. (1998).

Within the accuracy of the age models used to construct the climate records, high-latitude Northern Hemisphere D–O interstades can be hypothesized to have been accompanied by relatively warm and wet conditions over the western Great Basin between 46,000 and 27,000 GISP2 yr B.P. Sierran glacial advances occurred during D–O stades when the climate was relatively dry. However, our data are not sufficient to choose between competing hypotheses of climate change (Broecker et al., 1990; Bond et al., 1992; Broecker, 1994; Cane, 1998; Cane and Clement, 1999; Clark et al., 2001; Stott et al., 2002).

We suggest that the alternating cold/dry and warm/wet conditions that occurred in the western US between 46,000 and 21,000 GISP2 yr B.P. were directly related to the movement of the PJS. During stades, the mean position of the PJS lay south of 35°N, bringing cold and relatively dry conditions to the Sierra Nevada and western Great Basin. During interstades, the mean position of the PJS shifted north (between 35° and $\geq 43^\circ$N), greatly increasing the amount of precipitation received by Great Basin surface-water systems. In addition, warmer temperatures associated with the southern boundary of the PJS aided the retreat of Sierran alpine glaciers during interstades.

Climate records from sites that sample much of the Northern Hemisphere indicate that D–O cyclicity impacted much of the hemisphere, perhaps synchronously. The mechanism that begins and ends a D–O oscillation, and the teleconnections that transmit its effects throughout the Northern Hemisphere, are not well understood. We suggest that the data presented in this paper indicate that any theory that seeks to explain the mechanism and propagation of D–O cyclicity should also provide a mechanism that explains the spatial migration of the PJS during D–O oscillations.

## Acknowledgements

Julie Macie at the US Geological Survey performed the ostracode separations and Stephen Howe at the University at Albany-SUNY performed the $\delta^{18}$O analyses. We thank Richard Forester and Kelly Conrad of the US Geological Survey for their assistance with the ostracode study. We also thank Fred Phillips and one anonymous reviewer for their efforts. The senior author would like to acknowledge the Pyramid Lake Paiute Tribe and its Resources Group for their assistance in studies of Pyramid Lake.

## References


Altabet, M.A., Higginson, M.J., Murray, D.W., 2002. The effect of millennial-scale changes in Arabian Sea denitrification on atmospheric $CO_2$. Nature 415, 159–162.

Behl, R.J., Kennett, J.P., 1996. Brief interstadial events in the Santa Barbara basin, NE Pacific, during the past 60 kyr. Nature 379, 243–246.

Benson, L., 1999. Records of millennial-scale climate change form the Great Basin of the western United States. In: Clark, P., Webb, R., Keigwin, L. (Eds.), Mechanisms of Global Climate Change at Millennial Time Scales. American Geophysical Union Monograph, Vol. 112, pp. 203–225.

Benson, L.V., Thompson, R.S., 1987b. Lake-level variation in the Lahontan Basin for the past 50,000 years. Quaternary Research 28, 69–85.

Benson, L.V., Paillet, F.L., 2002b. HIBAL: a hydrologic–isotopic-balance model for application to paleolake systems. Quaternary Science Reviews 21, 1521–1539.

Benson, L.V., Burdett, J.W., Kashgarian, M., Lund, S.P., Phillips, F.M., Rye, R.O., 1996. Climatic and hydrologic oscillations in the Owens Lake basin and adjacent Sierra Nevada, California. Science 274, 746–749.

Benson, L.V., Smoot, J.P., Kashgarian, M., Sarna-Wojcicki, A., Burdett, J.W., 1997. Radiocarbon ages and environments of deposition of the Wono and Trego Hot Springs tephra layers in the Pyramid Lake subbasin, Nevada. Quaternary Research 47, 251–260.

Benson, L.V., May, H.M., Antweiler, R.C., Brinton, T.I., Kashgarian, M., Smoot, J., Lund, S.J., 1998a. Continuous lake-sediment records of glaciation in the Sierra Nevada between 52,600 and 12,500 $^{14}C$ yr B.P. Quaternary Research 50, 113–127.

Benson, L.V., Lund, S.P., Burdett, J.W., Kashgarian, M., Rose, T.P., Smoot, J., Schwartz, M.D., 1998b. Correlation of Late-Pleistocene lake level oscillations in Mono Lake, California, with North Atlantic climate events. Quaternary Research 49, 1–10.

Benson, L.V., Kashgarian, M., Rye, R.O., Lund, S.P., Paillet, F.L., Smoot, J., Kester, C., Mensing, S., Meko, D., Lindstrom, S., 2002a. Holocene multidecadal and multicentennial droughts affecting northern California and Nevada. Quaternary Science Reviews 21, 659–682.

Benson, L., Liddicoat, J., Smoot, J., Sarna-Wojcicki, A., Negrini, R., Lund, S., 2003. Age of the Mono Lake excursion and associated tephra. Quaternary Science Reviews 22, 135–140.

Benson, L., Linsley, B., Smoot, J., Mensing, S., Lund, S., Stine, S., Sarna-Wojcicki, A., 2003a. Influence of the Pacific Decadal Oscillation on the climate of the Sierra Nevada, California and Nevada. Quaternary Research 59, 151–159.

Bond, G., Heinrich, H., Broecker, W., Labeyrie, L., McManus, J., Andrews, J., Huon, S., Jantschik, R., Clasen, S., Simet, C., Tedesco, K., Klas, M., Bonani, G., Ivy, S., 1992. Evidence for massive discharges of icebergs into the North Atlantic Ocean during the last glacial period. Nature 360, 245–249.

Bond, G., Broecker, W., Johnsen, S., McManus, J., Labeyrie, L., Jouzel, J., Bonani, G., 1993. Correlations between climate records from North Atlantic sediments and Greenland ice. Nature 365, 143–147.

Boyle, E.A., 1997. Characteristics of the deep ocean carbon system during the past 150,000 years: SCO2 distributions, deep water flow patterns, and abrupt climate change. Proceedings of the National Academy of Science 94, 8300–8307.

Broecker, W.S., 1994. Massive iceberg discharges as triggers for global climate change. Nature 372, 421–424.

Broecker, W.S., Bond, G., Klas, M., Bonani, G., Wolfli, W., 1990. A salt oscillator in the glacial Atlantic? 1 The concept. Paleoceanography 5, 469–477.

Broecker, W.S., Bond, G., Klas, M., Clark, E., McManus, J., 1992. Origin of the northern Atlantic's Heinrich events. Climate Dynamics 1992, 265–273.

Cane, M.A., 1998. A role for the tropical Pacific. Science 282, 59–61.

Cane, M.A., Clement, A.C., 1999. A role for the tropical Pacific coupled ocean–atmosphere system on Milankovitch and millennial time scales. Part II: global impacts. In: Clark, P.U., Webb, R.S., Keigwin, L.D. (Eds.), Geophysical Monograph 112: Mechanisms of Global Climate Change at Millennial Time Scales. American Geophysical Union, Washington DC, pp. 373–383.

Clark, P.U., Marshall, S.J., Clarke, G.K., Hostetler, S., Licciardi, J.M., Teller, J.T., 2001. Freshwater forcing of abrupt climate change during the last glaciation. Science 293, 283–287.

Cohen, A.S., Palacios-Fest, M.R., Negrini, P.E., Wigand, P.E., Erbes, D.B., 2000. A paleoclimate record for the past 250,000 years from Summer Lake, Oregon, USA: III sedimentology, paleontology and geochemistry. Journal of Paleolimnology 24, 151–181.

Dansgaard, W., 1964. Stable isotopes in precipitation. Tellus 16, 436–468.

Dansgaard, W., Johnsen, S., Clausen, H.B., Dahl-Jensen, D., Gundestrup, N.S., Hammer, C.U., Hvidberg, C.S., Steffensen, J.P., Sveinbjornsdottir, A.E., Jouzel, J., Bond, G., 1993. Evidence for general instability of past climate from a 250-kyr ice-core record. Nature 364, 218–220.

Gentry, D., Blamart, D., Ouahdi, R., Gilmour, M., Baker, A., Jouzel, J., Van-Exter, S., 2003. Precise dating of Dansgaard–Oeschger climate oscillations in western Europe from stalagmite data. Nature 421, 833–837.

Grootes, P.M., Stuiver, M., 1997. Oxygen 18/16 variability in Greenland snow and ice with $10^{-3}$-to $10^5$-year time resolution. Journal of Geophysical Research 102, 26455–26470.

Heinrich, H., 1988. Origin and consequences of cyclic ice rafting in the Northeast Atlantic Ocean during the past 130,000 years. Quaternary Research 29, 142–152.

Hendy, I.L., Kennett, J.P., 1999. Latest Quaternary North Pacific surface-water responses imply atmosphere-driven climate instability. Geology 27, 291–294.

Hendy, I.L., Kennett, J.P., Roark, E.B., Ingram, B.L., 2002. Apparent synchroneity of submillennial scale climate events between Greenland and Santa Barbara Basin, California from 30–10 ka. Quaternary Science Reviews 21, 1167–1184.

Heusser, L., 1998. Direct correlation of millennial-scale changes in western North American vegetation and climate with changes in the California current system over the past ~60 kyr. Paleoceanography 13, 252–262.

Hinnov, L.A., Schulz, M., Yiou, P., 2002. Interhemispheric space-time attributes of the Dansgaard–Oeschger oscillations between 100 and 0 ka. Quaternary Science Reviews 21, 1213–1228.

Hostetler, S.W., Benson, L.V., 1990. Paleoclimatic implications of the high stand of Lake Lahontan derived from models of evaporation and lake level. Climate Dynamics 4, 207–217.

Hughen, K.A., Overpeck, J.T., Peterson, L.C., Trumbore, S., 1996. Rapid climate changes in the tropical Atlantic region during the last deglaciation. Nature 380, 51–54.

Johnsen, S., Clausen, H.B., Dansgaard, W., Fuhrer, K., Gundestrup, N.S., Hammer, C.U., Iversen, P., Jouzel, J., Stauffer, B., Steffensen, J.P., 1992. Irregular glacial interstadials recorded in a new Greenland ice core. Nature 359, 311–313.

Johnsen, S., Clausen, H.B., Dansgaard, W., Gundestrup, N.S., Hammer, C.U., Andersen, U., Andersen, K.K., Hvidberg, C.S., Dahl-Jensen, D., Steffensen, J.P., Shoji, H., Sveinbjornsdottir, A.E., White, J.W.C., Jouzel, J., Fisher, D., 1997. The $\delta^{18}O$ record along the Greeland Ice Core Project deep ice core and the problem of possible Eemian climate instability. Journal of Geophysical Research 102, 26397–26410.

Jouzel, J., Alley, R.B., Cuffey, K.M., Dansgaard, W., Grootes, P.M., Hoffman, G., Johnson, S.J., Koster, R.D., Peel, D., Shuman, C.A., Stievenard, M., Stuiver, M., White, J.C., 1997. Validity of the temperature reconstruction for water isotopes in ice cores. Journal of Geophysical Research 102, 26471–26487.

Kutzbach, J.E., Guetter, P.J., 1986. The influence of changing orbital parameters and surface boundary conditions on climate simulations for the past 18,000 years. Journal of Atmospheric Sciences 43, 1726–1759.

Laj, C., Kissel, C., Mazaud, A., Channell, J.E.T., Beer, J., 2000. North Atlantic palaeointensity stack since 75 ka (NAPIS-75) and the duration of the Laschamp event. Philosophical Transactions of the Royal Society of London A358, 1009–1025.

Lang, C., Leuenberger, M., Schwander, J., Johnsen, S., 1999. 16°C Rapid temperature variation in central Greenland 70,000 years ago. Science 286, 934–937.

Liddicoat, J.C., 1992. Mono Lake excursion in Mono Basin, California, and at Carson Sink and Pyramid Lake, Nevada. Geophysical Journal International 108, 442–452.

Lund, S.P., Liddicoat, J.C., Lajoie, K.R., Henyey, T.L., Robinson, S.W., 1988. Paleomagnetic evidence for long-term ($10^4$ year) memory and periodic behavior in the Earth's core dynamo process. Geophysical Research Letters 15, 1101–1104.

Manabe, S., Broccoli, A.J., 1985. The influence of continental ice sheets on the climate of an ice age. Journal of Geophysical Research 90, 2167–2190.

Negrini, R.M., Erbes, D.B., Faber, K., Herrera, A.M., Robers, A.P., Cohen, A.S., Wigand, P.E., Foit, F.F., 2000. A paleoclimate record for the past 250,000 years from Summer Lake, Oregon, USA: I chronology and magnetic proxies for lake level. Journal of Paleolimnology 24, 125–149.

O'Neil, J.R., Clayton, R.N., Mayeda, T.K., 1969. Oxygen isotope fractionation in divalent metal carbonates. Journal of Chemical Physics 51, 5547–5558.

Ooishi, W., 1926. Raporto de la Aerologia Observatorio de Tateno. Aerological Observatory Report 1, Central Meteorological Observatory, Japan, 213pp.

Peterson, L.C., Haug, G.H., Hughen, K.A., Röhl, U., 2000. Rapid changes in the hydrologic cycle of the Tropical Atlantic during the last glacial. Science 290, 1947–1951.

Pyke, C.B., 1972. Some meteorological aspects of the seasonal distribution of precipitation in the western United States and Baja California. University of California Water Resources Center Contribution 139.

Rasmussen, T.L., Thomsen, E., van Weering, T.C.E., Labeyrie, L., 1996. Rapid changes in surface and deep water conditions at the Faeroe Margin during the last 58,000 years. Paleoceanography 11, 757–771.

Riehl, H., Alaka, M.A., Jordan, C.L., Renard, R.J., 1954. The Jet Stream. Meteorological Monograph 2, 23–47.

Russell, I.C., 1884. A geological reconnaissance in southern Oregon. US Geological Survey Annual Report 4, 431–464.

Russell, I.C., 1885. Geological History of Lake Lahontan. US Geological Survey Monograph 11, 288pp.

Russell, I.C., 1889. Quaternary history of Mono Valley, California. US Geological Survey Annual Report 8, 261–394.

Sachs, J.P., Lehman, S.J., 1999. Covariation of subtropical and Greenland temperatures 60,000 to 30,000 years ago. Science 286, 756–759.

Seki, O., Ishiwatari, R., Matsumoto, K., 2002. Millennial climate oscillations in NE pacific surface waters over the last 82 kyr: new evidence from alkenones. Geophysical Research Letters 29, 59-1–59-4.

Severinghaus, J.P., Brook, E.J., 1999. Abrupt climate change at the end of the last glacial period inferred from trapped air in polar ice. Science 286, 930–934.

Severinghaus, J.P., Sowers, T., Brook, E.J., Alley, R.B., Bender, M.L., 1998. Timing of abrupt climate change at the end of the Younger Dryas interval from thermally fractionated gases in polar ice. Nature 391, 141–146.

Smith, G.I., Bischoff, J.L., Bradbury, J.P., 1997. Synthesis of the paleoclimatic record from Owens Lake core OL-92. In: Smith, G.I., Bischoff, J.L. (Eds.), An 800,000-Year Paleoclimatic Record from Core OL-92, Owens Lake, California. Geological Society of America Special Paper 317, pp. 143–160.

Starrett, L.G., 1949. The relation of precipitation patterns in North America to certain types of jet streams at the 300-millibar level. Journal of Meteorology 6, 347–352.

Stott, L., Poulsen, C., Lund, S., Thunell, R., 2002. Super ENSO and global climate oscillations at millennial time scales. Science 297, 222–226.

Stuiver, M., Grootes, P.M., 2000. GISP2 oxygen isotope ratios. Quaternary Research 53, 277–284.

Voelker, A.H., Sarnthein, M., Grootes, P.M., Erlenkeuser, H., Laj, C., Mazaud, A., Nadeau, M., Schleicher, M., 1998. Correlation of marine $^{14}C$ ages from the Nordic seas with the GISP2 isotope record: implications for $^{14}C$ calibration beyond 25 ka BP. Radiocarbon 40, 517–534.

Wagner, G., Beer, J., Laj, C., Kissel, C., Masarik, J., Muschele, R., Synal, H., 2000. Chlorine-36 evidence for the Mono Lake event in the Summit GRIP ice core. Earth and Planetary Science Letters 181, 1–6.

Wang, Y.J., Cheng, H., Edwards, R.L., An, Z.S., Wu, J.Y., Shen, C.-C., Dorale, J.A., 2001. A high-resolution absolute-dated late Pleistocene monsoon record from Hulu Cave, China. Science 294, 2345–2348.

Zic, M., Negrini, R.M., Wigand, P.E., 2002. Evidence of synchronous climate change across the Northern Hemisphere between the North Atlantic and the northwestern Great Basin. United States. Geology 30, 635–638.